MedChemComm

Cite this: *Med. Chem. Commun.*, 2012, **3**, 167

www.rsc.org/medchemcomm

CONCISE ARTICLE

Binding free energy calculations and biological testing of novel thiobarbiturates as inhibitors of the human NAD$^+$ dependent histone deacetylase Sirt2†

Urszula Uciechowska,[a] Jörg Schemies,[b] Michael Scharfe,[a] Michael Lawson,[a] Kanin Wichapong,[a] Manfred Jung[b] and Wolfgang Sippl*[a]

Received 19th August 2011, Accepted 27th October 2011
DOI: 10.1039/c1md00214g

A multi-step virtual screening was carried out in order to identify inhibitors of human NAD$^+$-dependent deacetylase sirtuin 2 (Sirt2). Molecular mechanics Poisson–Boltzmann surface area (MM-PB/SA) and linear interaction energy (LIE) calculations were carried out on a training set of ten recently identified Sirt2 inhibitors from our laboratory. The docking scores did not reproduce the relative binding free energies estimated from the *in vitro* data, while the LIE and the MM-PB/SA data were found to be in good agreement with the experimental data for the ten inhibitors. Both binding free energy methods were successful in predicting the activity of 14 novel identified thiobarbiturates and led to Sirt2 inhibitors that are ten-fold more active than those from the training set. The provided data obtained by the combination of docking and MD-based binding free energy calculations show the performance of the approach for predicting the binding free energy of novel sirtuin inhibitors.

Introduction

Computational methods are nowadays routinely used for discovery of new lead structures, and to understand the structural and energetic relationship between ligands and proteins. However, discovering novel bioactive compounds that bind to a target with a high affinity is still challenging. There are many approaches employed to predict the binding free energy of a small molecule to a protein target. Free energy perturbation (FEP) and thermodynamic integration (TI) methods have been successfully applied to reproduce experimentally determined binding free energies.[1,2] However, these approaches are computationally expensive. Docking programs on the other hand are fast and use simple scoring functions to predict the binding strength of ligands.[3–5] A vast number of docking/virtual screening studies have been published over the last few years which could show that these methods are able to provide novel hits. However, to date the scoring functions included in docking programs are too inaccurate to further optimize the identified hits.

Two approaches—molecular mechanics Poisson–Boltzmann surface area (MM-PB/SA)[6–8] and linear interaction energy (LIE)—have recently become of interest in drug discovery as alternatives for predicting relative binding free energies. The LIE approximation was first described and further extended by Aqvist *et al.*[9] The LIE derived binding free energies are estimated from molecular dynamics (MD) or Monte-Carlo (MC) simulations. The concept of this method is to separately evaluate the electrostatic and van der Waals interaction energies of the ligand in bound and free states. Thus, two MD simulations have to be performed: one with the ligand bound to receptor and one with the unbound ligand in solvent. The binding free energy is calculated as:

$$\Delta G_{\text{bind}} = \Delta G_{\text{sol}}{}^{\text{P}} - \Delta G_{\text{sol}}{}^{\text{W}} \quad (1)$$

where ΔG_{sol} denotes the solvation free energy of transferring ligand from the gas-phase to the different environments, protein and water. The solvation free energies are obtained as a sum of intermolecular electrostatic and van der Waals interactions. The averages of interaction energies between the ligand and its surroundings are obtained from the equation:

$$\Delta G_{\text{calc}} = \alpha \Delta E_{\text{vdw}} + \beta \Delta E_{\text{EL}} + \gamma \quad (2)$$

where ΔE_{vdw} describes the van der Waals interaction energy and ΔE_{EL} the electrostatic interaction energy of the ligand bound to the receptor and the ligand free in solution. α and β values are fitting parameters which were obtained by using linear regression analysis. The third term is a constant termed γ which sometimes

[a]*Department of Pharmaceutical Chemistry, Martin-Luther Universität Halle-Wittenberg, Wolfgang-Langenbeckstr. 4, 06120 Halle/Saale, Germany. E-mail: wolfgang.sippl@pharmazie.uni-halle.de; Fax: +49-345-55-27355; Tel: +49-345-55-25040*
[b]*Institute of Pharmaceutical Sciences, Albert-Ludwigs-Universität, Freiburg, Germany*

† Electronic supplementary information (ESI) available: Computational methods and experimental procedures (*in vitro* screening). See DOI: 10.1039/c1md00214g

needs to be included in order to obtain a reasonable correlation. Another very common method for calculating binding free energy values is the MM-PB/SA approach, pioneered by Kollman *et al.*[7] The MM-PB/SA approach has been applied in many different areas, *e.g.* the study of the stability of DNA binders,[10] or the estimation of the binding free energies of protein–ligand complexes.[3,11]

Histone deacetylases (HDACs) are transcriptional regulators that deacetylate histones but also a high number of other non-histone proteins. The enzymatic activity affects the conformational state and the activities of the substrate proteins. Four classes of histone deacetylases have been described in humans: classes I, II and IV have been shown to be zinc dependent amidohydrolases and eleven subtypes have been described (HDAC1-11).[12] Class III enzymes rely in their catalysis on the cofactor NAD^+. Based on the homology to the yeast histone deacetylase Sir2p the NAD^+-dependent deacetylases have been termed sirtuins and seven members (Sirt1–7) have been identified in humans.[13] Whereas class I, II and IV histone HDACs have been identified as valid anticancer targets and two inhibitors have been approved for clinical use,[14] much less is known about the consequences of class III HDAC inhibition.[13] Sirtuins have been linked to aging and overexpression of sirtuins leads to a prolonged lifespan in yeast.[15] More recently, sirtuins activity has been tied to the pathogenesis of HIV[16] and cancer[17–19] and also neurological diseases.[20] Only a limited number of sirtuin inhibitors is known and some of them do not inhibit human subtypes.[21–29] (For review see ref. 21 and 22.) Recently, we identified thiobarbiturates as novel class of sirtuin inhibitiors.[30]

The aim of this work was to identify more active thiobarbiturates as sirtuin inhibitors by virtual screening of large compound libraries. In addition we were interested to compare and apply two MD based binding free energy calculation methods, MM-PB/SA and linear interaction energy (LIE), respectively. The ensemble averages derived from MD simulation were used for calculating enthalpy and entropy terms for MM-PB/SA as well as E_{vdw} and E_{ele} energies for the LIE model. The derived binding free energy models were applied to evaluate the inhibitory activity of unknown compounds selected from a virtual screening on Sirt2.

Results

Virtual screening

Based on our recently identified thiobarbiturates as Sirt2 inhibitors we conducted a further virtual screening (VS) using the Chembridge database in order to find more potent compounds.[30,31] MACCS key fingerprints were used to search the Chembridge database for compounds similar to the most active thiobarbiturates from our previous work (compounds **3** and **6**, Fig. 1).[30] This resulted in 637 compounds which were subsequently filtered by applying the following criteria: $M_w > 500$, log $P < 4$, topological polar surface area TPSA < 140 Å.[2] The resulting 510 molecules were docked in the Sirt2 binding pocket using the GOLD program.[32] The human Sirt2 crystal structure (monomer B)[33] was used for the docking study as previously described.[30] 129 compounds showed a Goldscore higher than 40 and were further analyzed using calculated molecular interaction

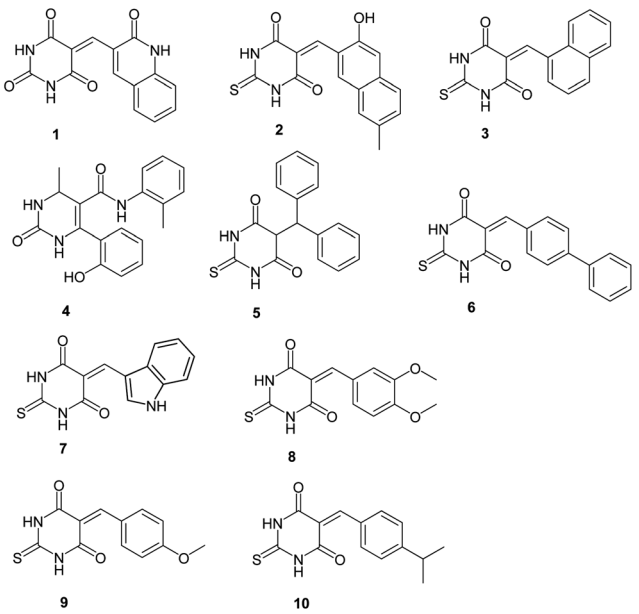

Fig. 1 Thiobarbiturates and barbiturates used as the training set (taken from ref. 30).

fields of the Sirt2 binding pocket. 14 thiobarbiturate derivatives were manually selected after visual inspection of their binding mode and their biological data were predicted using binding free energy calculations (Fig. 2).

All docked thiobarbiturate compounds showed the same binding mode as exemplarily shown for compound **16** (Fig. 3). The binding mode is in agreement with results for compounds **3** and **6**, as recently reported.[30] Hydrogen bonds were detected with the polar residues Asn168, His187 and the water molecules. The hydrophobic parts of the molecules interact with the acetyl lysine channel including the amino acids Phe119, His187, Val233 and Phe234. The 14 compounds were tested in a Sirt2 *in vitro* assay and showed inhibition in the low micromolar range (1.5–5.8 μM, Table 1). The most active compounds with IC_{50} values around 1 μM showed favourable hydrophobic interactions in the acetyl lysine channel. Calculated molecular interaction fields using a hydrophobic methyl probe supported the importance of the hydrophobic interactions in the acetyl lysine channel (Fig. S1, ESI†). Molecular dynamics simulations which were carried out for all compounds showed that the Sirt2-inhibitor complexes are stable with low root mean square deviation (RMSD) values (Fig. S2, ESI†).

Binding free energy calculations

Two different approaches, namely MM-PB/SA[34] and LIE,[9] were applied for estimating the binding free energy of the compounds under study. For evaluating the accuracy of different binding free energy approaches (MM-PB/SA and LIE) ten thiobarbiturate compounds developed in our laboratory were considered for model generation.[30] Subsequently, the derived models were used for predicting the activities of the novel compounds identified by virtual screening of the Chembridge compound collection.

The 14 novel thiobarbiturates were tested in an *in vitro* Sirt2 assay as described in the ESI†. All compounds gave IC_{50} values

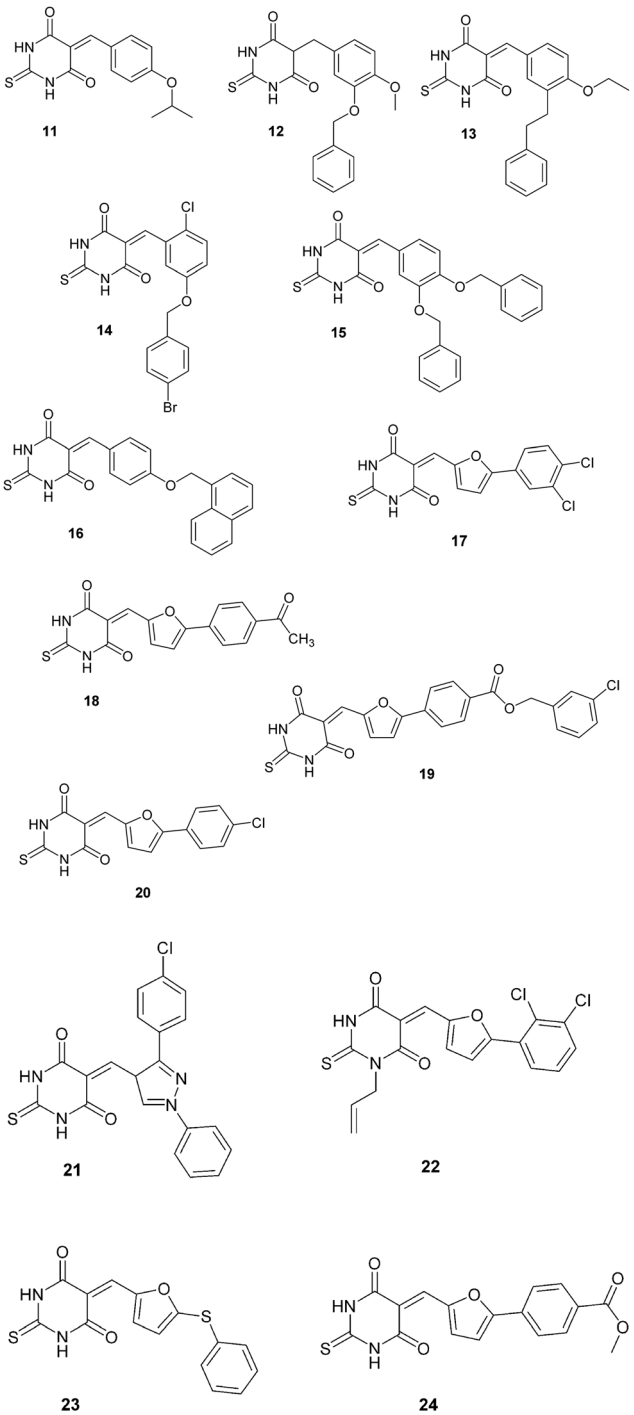

Fig. 2 14 candidates found in virtual screening were used as the test set in this study.

in the range between 6 and 1 μM, which is below the range observed for the first series of thiobarbiturates (Table 1).

MM-PB/SA calculations

The MD trajectories from the end of the simulation time were used to apply the MM-PB/SA method (see ESI† for further details). The absolute free energy of a system is estimated from a combination of molecular mechanics, *i.e.* Poisson–Boltzmann

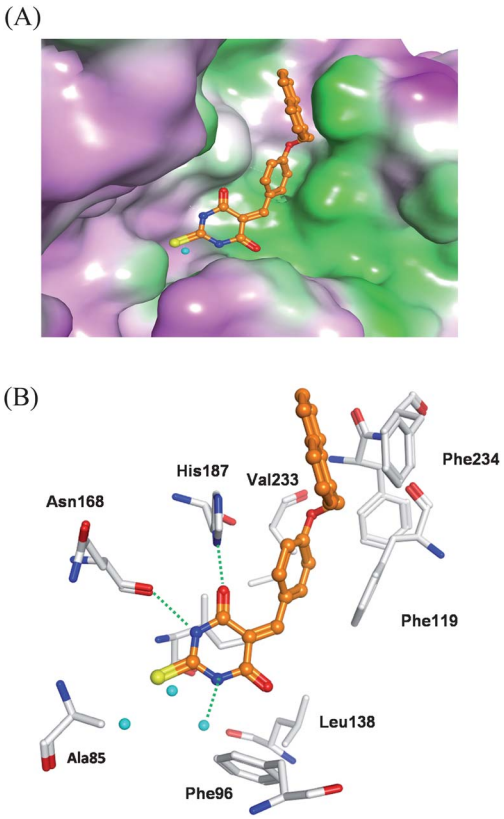

Fig. 3 Predicted docking pose for compound **16** (coloured orange). (A) The molecular surface of the Sirt2 binding pocket is displayed and coloured according to the hydrophobicity (magenta = hydrophilic, green = hydrophobic). (B) Interacting amino acids are displayed. Hydrogen bonds are shown as green dashed lines. Water molecules are shown as cyan coloured balls.

estimation of the electrostatic free energy determined from the exposed surface area, and an estimate of the entropy of the system derived from normal mode calculations (Table S1, ESI†). The correlation between ΔG_{exp} and predicted ΔG values was expressed in terms of the square of the correlation coefficient (r^2). The ΔG model was generated by using ten compounds as a training set as shown in Fig. 1 and gave a correlation coefficient of $r^2 = 0.54$ and a root mean square error (RMSE) of 0.24 kcal mol^{-1} (Fig. 4). In the same way the calculated enthalpy of binding values (ΔH) were fitted with the experimental ΔG_{exp} values (Table 1). For this model the correlation coefficient was slightly higher ($r^2 = 0.61$, RMSE = 0.22 kcal mol^{-1}) as shown in Fig. 5A. Compound **10** was found to be an outlier because the difference between calculated and experimental values is high in comparison to the other compounds. The MD simulation of compound **10** showed larger RMSD values as a consequence of larger adaption of the protein to the inhibitor. As a consequence the final ΔH value of this compound was significantly higher compared to the other similar compounds. Therefore this compound was excluded from the model generation. Excluding it resulted in a significantly better correlation ($r^2 = 0.76$ and RMSE of 0.18 kcal mol^{-1}) (Fig. 5B). The leave-one-out cross-validation coefficient r^2_{LOO} was calculated as 0.64 indicating the robustness of the reduced model. Therefore, the reduced dataset was used for the prediction of the compounds identified by the virtual screening.

Table 1 Predicted biological data for the 14 novel compounds, $pIC_{50}pred\Delta H$—values predicted using the ΔH model, $pIC_{50}pred\Delta G$—values predicted using the ΔG model, pIC_{50}—experimental data, error difference between experimental and calculated values

Cpd	Chembridge name	IC50 Sirt2/μM	pIC_{50}	$pIC_{50}pred\Delta H$	Error	$pIC_{50}pred\Delta G$	Error
11	6486096	5.8 ± 0.4	5.23	5.32	0.09	5.02	0.21
12	5851689	5.8 ± 0.9	5.23	5.47	0.24	4.29	0.94
13	5860305	4.9 ± 0.5	5.30	5.38	0.08	4.48	0.82
14	6446861	1.8 ± 0.6	5.74	5.60	0.14	4.84	0.90
15	6218896	3.9 ± 0.3	5.40	5.90	0.50	4.90	0.50
16	5680998	2.6 ± 0.9	5.58	5.64	0.06	5.60	0.02
17	5545264	1.5 ± 0.4	5.82	5.59	0.23	4.93	0.89
18	6568425	5.5 ± 1.3	5.26	5.62	0.36	5.33	0.07
19	5483251	2.2 ± 0.1	5.19	5.31	0.12	5.03	0.16
20	7093707	6.5 ± 0.5	5.66	5.66	0.00	5.20	0.46
21	5875121	3.8 ± 0.3	5.42	5.55	0.13	5.46	0.04
22	5966223	2.8 ± 0.5	5.55	5.65	0.10	5.03	0.52
23	6060663	3.5 ± 0.4	5.46	5.54	0.08	5.06	0.40
24	6194121	5.7 ± 0.5	5.24	5.54	0.30	5.18	0.06

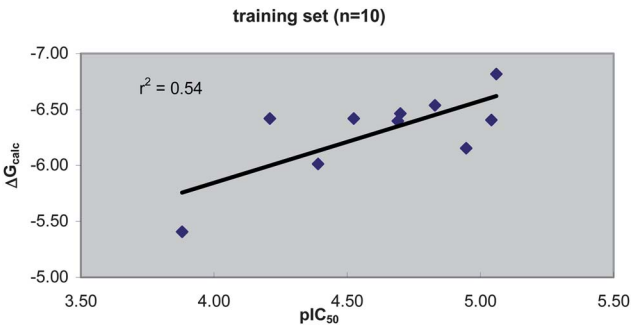

Fig. 4 Correlation between experimental pIC_{50} values and calculated ΔG values from the MM-PB/SA model. Training set, $n = 10$.

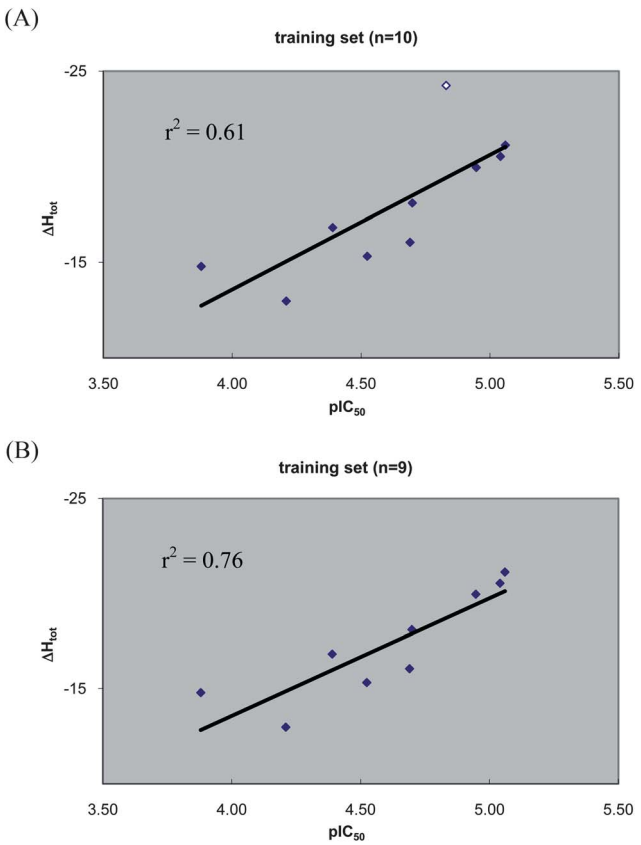

Fig. 5 Correlation between experimental pIC_{50} values and calculated ΔH_{tot} values from the MM-PB/SA model. (A) Training set, $n = 10$. (B) Outlier removed. Training set, n=9.

The MM-PB/SA derived ΔG and ΔH models were applied to predict the affinities for the test set compounds $n = 14$ (Fig. 2). The predicted values using the ΔG model were found to be quite far away from the ΔG_{exp} values, thus resulting in a large deviation of the residual values (~0.9 log units for compounds **12**, **14** and **17**) (see Table 1). The ΔG model gave a correlation coefficient of prediction $r^2_{PRED} = 0.78$ for the 14 test set compounds and an overall r^2 value of 0.60 (data not shown). However, it has to be stated that the training set and the test activities set are quite different. In the training set pIC_{50}-values are between 3.88 and 5.04 while in the test set between 5.19 and 5.74. On the other hand, the enthalpy model ΔH showed excellent results (Table 1) with an $r^2_{PRED} = 0.96$ for the 14 test set compounds and an overall $r^2 = 0.80$ for all 24 compounds (Fig. 6). The maximum error observed here was 0.50 log units for compound **15**. Upon comparison of the two models it is obvious that the ΔH model was accurate for predicting the test set molecules and that the problem of the ΔG model lies in the entropy change upon binding. In general, entropy calculation is a difficult task especially if the conformational fluctuations are significant.[11]

LIE calculations

Based on MD simulations the electrostatic and van der Waals interactions were calculated to solve the binding free energy equation (eqn (1) and (2)). The experimental data were then fitted with the calculated binding energy to obtain ΔG predicted values listed in Table 3. The empirical parameters α, β and constant γ were determined using the least-square error fitting method within the MOE program and solved in a fashion similar to that of QSAR models. Two models were prepared: model (1), where α, β and γ parameters were evaluated, and model (2), where only α and β were evaluated and γ was set to zero.

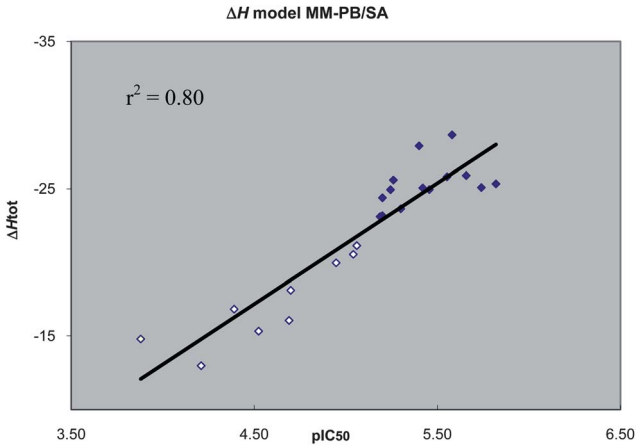

Fig. 6 Correlation between experimental pIC_{50} values and calculated ΔH values for training and test set thiobarbiturates (outlier from Fig. 5A removed). Training set molecules are coloured white.

Based on the results from training set compounds and the three parameter equation, two models were estimated, model 1 (eqn (3)) and model 2 (eqn (4)):

$$\Delta G_{\text{binding}} = 0.14(E_{\text{vdW}}) - 0.11(E_{\text{ele}}) - 3.98 \quad (3)$$

$$\Delta G_{\text{binding}} = 0.36(E_{\text{vdW}}) - 0.17(E_{\text{ele}}) + 0 \quad (4)$$

For model 1 (Fig. 7A and Table 2) correlation between ΔG_{exp} and predicted ΔG values was $r^2 = 0.74$ with an RMSE of 0.25. The second model described with eqn (4) gave a lower correlation with an $r^2 = 0.58$ and an RMSE of 0.32 (Fig. 7B and Table 2). Thus, the models showed comparable statistical values as the MM-PB/SA ΔH model. In addition, the two LIE models were applied to predict the binding free energy of the 14 test set compounds, in order to see whether comparable accuracy as observed for the MM-PB/SA model could be derived. The LIE model 1 gave a correlation coefficient of $r^2_{\text{PRED}} = 0.68$ for the test set compounds and an overall correlation coefficient of $r^2 = 0.47$ for all 24 compounds (Fig. 8A). The LIE model 2 which showed a lower correlation for the training set showed a higher r^2_{PRED} value of 0.72 for the test set and an overall $r^2 = 0.62$ for all

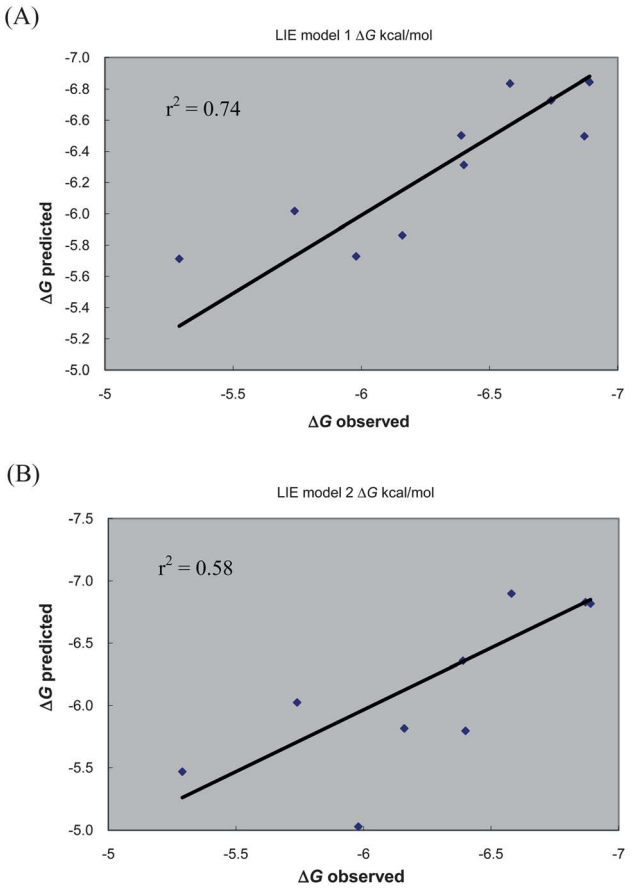

Fig. 7 Correlation between experimental pIC_{50} values and calculated ΔG_{LIE} values obtained from the (A) LIE model 1 and (B) LIE model 2. Training set, $n = 10$.

24 compounds (Fig. 8B). These results suggest that the LIE models were not as accurate in predicting the biological activities of the 14 novel compounds as observed for the MM-PB/SA ΔH model. Table 3 shows the calculated van der Waals and electrostatic energies for the compounds of the test set as well as the predicted activities. It is obvious that the favourable van der Waals energy of the most active compounds compensates the

Table 3 Overview of the electrostatics (ΔE_{ele}) and van der Waals (ΔE_{vdw}) energies (kcal mol^{-1}) obtained for a test set $n = 14$, ($\Delta G_{\text{LIE}}1$) values predicted with a fitting parameter $\gamma \neq 0$, and ($\Delta G_{\text{LIE}}2$) with a fitting parameter $\gamma = 0$, (ΔG_{exp}) experimental values

Ligand-surrounding interactions/kcal mol^{-1}					Prediction			
Cpd	$E_{\text{vdw-bound}}$	$E_{\text{vdw-free}}$	$E_{\text{ele-bound}}$	$E_{\text{ele-free}}$	$\Delta G_{\text{LIE}}1$	$\Delta G_{\text{LIE}}2$	pIC_{50}	ΔG_{exp}
11	−40.29	−22.79	−26.64	−26.89	−6.46	−6.34	5.23	−7.11
12	−50.78	−34.48	−26.26	−27.60	−6.38	−6.04	5.23	−7.11
13	−51.28	−28.61	−36.35	−31.27	−6.54	−7.30	5.30	−7.21
14	−43.71	−23.13	−34.46	−33.98	−6.80	−7.33	5.74	−7.80
15	−55.82	−34.51	−27.02	−26.54	−6.91	−7.59	5.40	−7.34
16	−51.28	−28.17	−36.35	−34.75	−7.02	−8.05	5.58	−7.59
17	−46.61	−23.87	−29.14	−29.32	−7.19	−8.22	5.82	−7.91
18	−42.53	−21.09	−50.72	−48.57	−6.73	−7.36	5.26	−7.15
19	−52.85	−30.73	−39.09	−43.50	−7.61	−8.71	5.19	−7.05
20	−39.25	−20.91	−42.32	−40.22	−6.30	−6.25	5.66	−7.69
21	−52.01	−25.25	−39.22	−32.71	−6.94	−8.52	5.42	−7.36
22	−48.93	−26.43	−32.49	−30.92	−6.94	−7.83	5.55	−7.54
23	−43.25	−17.07	−38.40	−34.78	−7.21	−8.81	5.46	−7.41
24	−45.10	−23.48	−50.81	−48.71	−6.75	−7.42	5.24	−7.12

Table 2 Overview of the electrostatics (ΔE_{ele}) and van der Waals (ΔE_{vdw}) energies (kcal mol^{-1}) obtained for a training set $n = 10$, ($\Delta G_{LIE}1$) values predicted with a fitting parameter $\gamma \neq 0$, and ($\Delta G_{LIE}2$) with a fitting parameter $\gamma = 0$, (ΔG_{exp}) experimental values

	Ligand-surrounding interactions/kcal mol^{-1}				LIE models			
Cpd	$E_{vdw\text{-}bound}$	$E_{vdw\text{-}free}$	$E_{ele\text{-}bound}$	$E_{ele\text{-}free}$	$\Delta G_{LIE}1$	$\Delta G_{LIE}2$	pIC_{50}	ΔG_{exp}
1	−38.18	−18.70	−42.47	−36.73	−6.02	−6.03	4.21	−5.75
2	−43.98	−21.33	−32.62	−29.25	−6.73	−7.58	4.95	−6.74
3	−37.53	−17.54	−27.52	−25.35	−6.50	−6.83	5.04	−6.87
4	−39.78	−20.92	−38.92	−31.27	−5.71	−5.47	3.88	−5.29
5	−35.98	−20.19	−29.85	−26.03	−5.73	−5.03	4.39	−5.98
6	−38.91	−22.49	−23.74	−28.88	−6.84	−6.82	5.06	−6.90
7	−35.03	−18.20	−23.53	−25.21	−6.50	−6.36	4.69	−6.40
8	−36.34	−16.70	−34.04	−26.76	−5.86	−5.82	4.52	−6.16
9	−32.21	−17.21	−26.14	−28.36	−6.31	−5.80	4.70	−6.41
10	−35.95	−18.89	−25.20	−29.50	−6.83	−6.90	4.83	−6.59

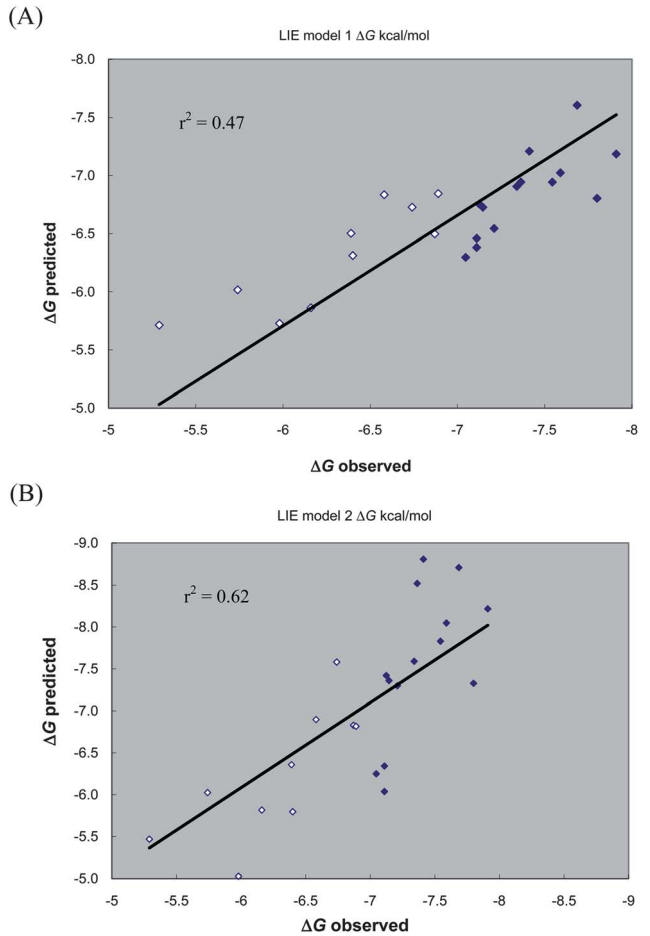

Fig. 8 Correlation between experimental pIC_{50} and calculated ΔG values for all 24 compounds. (A) LIE model 1 and (B) LIE model 2.

unfavourable effects of the electrostatic interactions, causing that the interaction is predominantly driven by van der Waals forces.

Conclusions

In the present study, novel thiobarbiturates were identified as Sirt2 inhibitors through a combination of virtual screening, binding free energy calculations and *in vitro* assaying. Docking potential VS hits to the Sirt2 binding site and subsequently carrying out MD simulations resulted in stable protein–ligand complexes. Their binding affinities were computed with MM-PB/SA and LIE approaches, respectively, in order to analyse the efficiency of their obtained models. In the case of the MM-PB/SA approach, two models either based on ΔG or ΔH were generated for predicting the binding free energy of test set compounds. The ΔH model showed an excellent predictive power, indicated by a high correlation coefficient and low RMSE values. Additionally, the model was able to correctly predict the activities of thiobarbiturates which were more than 10-fold more active than the ones included in the training set. So, even when the activity range of initial training set molecules and the novel thiobarbiturates used as the test set was quite different, the ΔH model was able to predict the new compounds to be more active than the original ones. Thus the model was not only able to predict the data of compounds with similar activities, but also able to detect more activities among the test set compounds. The ΔH MM-PB/SA model also correctly predicted the two most active compounds (**14** and **17**, Table 1). On the other hand, the ΔG model gave a lower correlation coefficient for the training set and also showed a reduced accuracy in predicting the activities of the test set compounds. Thus, the inclusion of the entropic term did not improve the statistical quality of the MM-PB/SA model.

The LIE models were also tested with the same dataset of Sirt2 inhibitor candidates. Two models were generated with either two or three parameters. It was shown that the model derived from the three-parameter equation gave higher correlation coefficients and lower RMSE values of the training set in comparison to the two-parameter model. Results revealed that the estimated binding free energies using the two-parameter model are closer to ΔG_{exp} than using the three-parameter model. Moreover the statistical values r^2_{PRED} and the correlation coefficient are also slightly better for the two-parameter model. However, in comparison to the MM-PB/SA ΔH model, the LIE models were not able to accurately predict the 14 test set compounds.

In summary, we have successfully combined docking and binding free energy calculations for finding, analysing and predicting binding affinities of new Sirt2 inhibitor candidates. The models were able to identify novel, more potent thiobarbiturates using a small training-set of 10 compounds. The computationally less demanding LIE models were also able to estimate the potency of the training set molecules, even with lower accuracy as

the MM-PB/SA ΔH model. Sirtuin inhibitors with increased potency are now optimized candidates for structure–activity studies by bioguided organic synthesis and interesting drug candidates for cancer and neurodegenerative disease.

Acknowledgements

This work was supported by the Deutsche Forschungsgemeinschaft (Si 868/6-1 and Ju 275/8-1). M.L. would like to acknowledge financial support from the German Fulbright Kommission and IIE.

References

1 M. Mezei, S. Swaminathan and D. L. Beveridge, *J. Am. Chem. Soc.*, 1978, **100**, 3255–3256.
2 D. L. Beveridge and F. M. DiCupa, *Annu. Rev. Biophys. Biophys. Chem.*, 1989, **18**, 431–492.
3 H. Gohlke and G. Klebe, *Angew. Chem., Int. Ed.*, 2002, **41**, 2644–2676.
4 G. L. Warren, C. W. Andrews, A.-M. Capelli, B. Clarke, J. LaLonde, M. H. Lambert, M. Lindvall, N. Nevins, S. F. Semus, S. Senger, G. Tedesco, I. D. Wall, J. M. Woolven, C. E. Peishoff and M. S. Head, *J. Med. Chem.*, 2006, **49**, 5912–5931.
5 P. Ferrara, H. Gohlke, D. J. Price, G. Klebe and C. L. Brooks, III, *J. Med. Chem.*, 2004, **47**, 3032–3047.
6 W. Wang and P. A. Kollman, *Proc. Natl. Acad. Sci. U. S. A.*, 2001, **98**, 14937–14942.
7 P. A. Kollman, I. Massova, C. Reyes, B. Kuhn, S. Huo, L. Chong, M. Lee, T. Lee, Y. Duan, W. Wang, O. Donini, P. Cieplak, J. Srinivasan, D. A. Case and T. E. Cheatham, *Acc. Chem. Res.*, 2000, **33**, 889–897.
8 T. Laitinen, J. A. Kankare and M. Perakyla, *Proteins*, 2004, **55**, 34–43.
9 J. Aqvist, C. Medina and J. E. Samuelsson, *Protein Eng.*, 1994, **7**, 385–391.
10 J. Srinivasan, T. E. Cheatham, P. Cieplak, P. A. Kollman and D. A. Case, *J. Am. Chem. Soc.*, 1998, **120**, 9401–9409.
11 H. Gohlke and D. A. Case, *J. Comput. Chem.*, 2004, **25**, 238–250.
12 C. M. Grozinger and S. L. Schreiber, *Chem. Biol.*, 2002, **9**, 3–16.
13 B. J. North and E. Verdin, *Genome Biol.*, 2004, **5**, 224.
14 R. W. Johnstone, *Nat. Rev. Drug Discovery*, 2002, **1**, 287–299.
15 S. Imai, C. M. Armstrong, M. Kaeberlein and L. Guarente, *Nature*, 2000, **403**, 795–800.
16 S. Pagans, A. Pedal, B. J. North, K. Kaehlcke, B. L. Marshall, A. Dorr, C. Hetzer-Egger, P. Henklein, R. Frye, M. W. McBurney, H. Hruby, M. Jung, E. Verdin and M. Ott, *PLoS Biol.*, 2005, **3**, e41.
17 H. Vaziri, S. K. Dessain, E. Ng Eaton, S. I. Imai, R. A. Frye, T. K. Pandita, L. Guarente and R. A. Weinberg, *Cell*, 2001, **107**, 149–159.
18 O. R. Bereshchenko, W. Gu and R. Dalla-Favera, *Nat. Genet.*, 2002, **32**, 606–613.
19 H. Ota, E. Tokunaga, K. Chang, M. Hikasa, K. Iijima, M. Eto, K. Kozaki, M. Akishita, Y. Ouchi and M. Kaneki, *Oncogene*, 2005, **25**, 176–185.
20 T. F. Outeiro, E. Kontopoulos, S. Altman, I. Kufareva, K. E. Strathearn, A. M. Amore, C. B. Volk, M. M. Maxwell, J. C. Rochet, P. J. McLean, A. B. Young, R. Abagyan, M. B. Feany, B. T. Hyman and A. Kazantsev, *Science*, 2007, **317**, 516–519.
21 M. Biel, V. Wascholowski and A. Giannis, *Angew. Chem.*, 2005, **117**, 3248–3280; M. Biel, V. Wascholowski and A. Giannis, *Angew. Chem., Int. Ed.*, 2005, **44**, 3186–3216.
22 M. Lawson, U. Uciechowska, J. Schemies, T. Rumpf, M. Jung and W. Sippl, *Biochim. Biophys. Acta, Gen. Subj.*, 2010, **1799**, 726–739.
23 A. J. Tervo, S. Kyrylenko, P. Niskanen, A. Salminen, J. Leppanen, T. H. Nyronen, T. Jarvinen and A. Poso, *J. Med. Chem.*, 2004, **47**, 6292–6298.
24 A. J. Tervo, T. Suuronen, S. Kyrylenko, E. Kuusisto, P. H. Kiviranta, A. Salminen, J. Leppanen and A. Poso, *J. Med. Chem.*, 2006, **49**, 7239–7241.
25 B. Heltweg, T. Gatbonton, A. D. Schuler, J. Posakony, H. Li, S. Goehle, R. Kollipara, R. A. Depinho, Y. Gu, J. A. Simon and A. Bedalov, *Cancer Res.*, 2006, **66**, 4368–4377.
26 J. Trapp, R. Meier, D. Hongwiset, M. U. Kassack, W. Sippl and M. Jung, *ChemMedChem*, 2007, **2**, 1419–1431.
27 D. Rotili, D. Tarantino, V. Carafa, E. Lara, S. Meade, G. Botta, A. Nebbioso, J. Schemies, M. Jung, A. G. Kazantsev, M. Esteller, M. F. Fraga, L. Altucci and A. Mai, *ChemMedChem*, 2010, **5**, 674–677.
28 J. Trapp, A. Jochum, R. Meier, L. Saunders, B. Marshall, C. Kunick, E. Verdin, P. G. Goekjian, W. Sippl and M. Jung, *J. Med. Chem.*, 2006, **49**, 7307–7316.
29 J. Posakony, M. Hirao, S. Stevens, J. A. Simon and A. Bedalov, *J. Med. Chem.*, 2004, **47**, 2635–2644.
30 U. Uciechowska, J. Schemies, R. Neugebauer, E. Huda, M. Schmitt, R. Meier, E. Verdin, M. Jung and W. Sippl, *ChemMedChem*, 2008, **3**, 1965–1976.
31 R. C. Neugebauer, U. Uchiechowska, R. Meier, H. Hruby, V. Valkov, E. Verdin, W. Sippl and M. Jung, *J. Med. Chem.*, 2008, **51**, 1203–1213.
32 G. Jones, P. Willett, R. C. Glen, A. R. Leach and R. Taylor, *J. Mol. Biol.*, 1997, **267**, 727–748.
33 M. S. Finnin, J. R. Donigian and N. P. Pavletich, *Nat. Struct. Biol.*, 2001, **8**, 621–625.
34 J. Wang, R. M. Wolf, J. W. Caldwell, P. A. Kollman and D. Case, *J. Comput. Chem.*, 2004, **25**, 1157–1174.